

Segmentation and Interpretation of MR Brain Images using an Improved Knowledge-Based Active Shape Model

Nicolae Duta², Milan Sonka¹

¹ Department of Electrical and Computer Engineering

² Department of Computer Science, The University of Iowa, Iowa City, IA 52242

Abstract. An improvement of the *Active Shape* procedure introduced by Cootes and Taylor is presented. The new automated brain segmentation and interpretation approach incorporates *a priori* knowledge about neuroanatomic structures and their specific structural relationships to provide robust segmentation and labeling.

The method was trained in 8 MR brain images and tested in 19 brain images by comparison to observer-defined independent standards. Neuroanatomic structures in all images from the test set were successfully identified. The presented method is applicable to virtually any task involving deformable shape analysis.

1 Introduction

The goal of our work reported here is to improve the *Active Shape* procedure introduced by Cootes and Taylor [1,2] to find new examples of previously learned shapes using the point distribution models. This approach is particularly useful in medical image analysis since human organs are not rigid and the variations in shape and appearance are difficult to model.

Automatic detection of brain structures is motivated by an ongoing effort to advance knowledge about relationships between anatomy and mental diseases in human brains. To date, most of the image segmentation in neuroscientific studies that utilize CT, MR, or PET rely on manual tracing. Despite the substantial interest and effort in the development of automated methods to identify brain structures, no reliable automated tools are available to date. The automated brain segmentation and interpretation approach described below represents a novel approach that incorporates *a priori* knowledge about neuroanatomic structures and their specific structural relationships to provide robust segmentation and labeling.

2 PDM Approach to MR Brain Image Interpretation

In many areas of image segmentation and interpretation, reliable a priori knowledge is available to help guide the image analysis process. For instance, in brain

imaging, the image data are routinely represented in a normalized Talairach space. Consequently, approximate positions of individual neuroanatomic structures can be determined. Knowledge about their sizes, shapes, gray level appearance, etc. can be acquired from a training set of examples.

2.1 Knowledge-Based Point Distribution Model

In order to improve the shape model and to take advantage of the available a priori knowledge, three additional features characteristic to MR brain images were included in the model: Gray-level appearance, border strength, and average position. In the implementation described below, we also used the implicit knowledge about object context representing inter-relationships of several objects and the fact that all objects of interest were always present in the image we search, a condition not applicable generally but appropriate for our application.

Gray-level appearance is calculated in neighborhoods around each of the shape model points. It is determined for every shape model point j of each training image along a profile g_j of a constant length, centered at the point j . Since the profiles vary with gray level scaling, derivatives of the gray levels along each profile are determined and normalized.

Border strength is determined for each border segment of the model. Every two consecutive model points that lie on the object boundary define a border segment. To compute its strength, a local filtering is applied to each clique on that border segment. The filter is based on a pair of close parallel profiles.

Average position of each shape model point that is calculated in the image coordinates is also incorporated in the model.

Our **knowledge-based shape model** combines generally applicable parameters of the point distribution model and the knowledge-specific parameters appropriate for the image segmentation task in question. As such, the complete model is composed of:

1. The eigenvectors corresponding to the largest eigenvalues of the covariance matrix describing the *Allowable Shape Domain* [1,2].
2. The average gray level appearance values for each point of the model.
3. The average border strength for corresponding border segments and the parameters of the mask (width, length) for which the strength was computed.
4. The average position of the points of the average shape.
5. Connectivity information (the number of shapes, point ordering along contours).

2.2 Searching for Objects: Model Fitting

The searching procedure developed for our PDM approach to image segmentation and interpretation is based on the model fitting strategy that substantially differs from the *Active Shape Procedure* of Cootes and Taylor. The difference is twofold. First, our search is entirely model driven meaning that segmentation hypotheses are not influenced by possibly misleading image data and do not use

any preprocessing. At each step of the fitting process, several model location hypotheses are considered and evaluated. Second, an outlier detection and replacement procedure has been developed to detect misplaced points and infer their new positions. The outlier detection improves robustness and accuracy of the shape model fitting process. The searching procedure consists of the following steps: 1) Model fitting using linear transforms, 2) model fitting using piecewise linear transforms, 3) outlier removal, 4) final point adjustment, 5) final outlier removal.

Model Fitting Function As a result of the hypotheses generation processes, shape model locations are sequentially hypothesized. In order to evaluate the model location hypotheses, a *fitness function* is needed to assess the agreement between the image data and the particular model instance. We have designed a *fitness function* $F = F_B/(F_{GA})^2$ that consists of two components:

1. *Fitness of the gray level appearance* F_{GA} is determined as the average squared Euclidean distance between the actual gray level appearance and the mean gray level profile incorporated in the shape model.
2. *Fitness of the border* F_B is calculated as the ratio between the aggregate response of all four point cliques along the contour and the maximum possible response (twice the number of cliques).

Model fitting using linear transforms Shape instance hypotheses specify the locations of all model points within the analyzed image. The hypotheses are generated using affine transformations and are applied to the model average position. All generated hypotheses are sequentially evaluated using the model fitting function F and the best fit is determined.

Model fitting using piecewise linear transforms Since non-rigid objects or object with inter-subject variability are discussed here, rigid linear transforms do not account for any potential deformations of the expected shape. Therefore, affine transforms are applied to subsets of 5–7 consecutive model points.

Outlier removal Under unfavorable circumstances, the previous step may introduce incorrectly determined vertices – **outliers**. This may happen if a sub-shape fitted by the previous step exhibits weak edges or if there exists another border of similar properties in the neighborhood. In the existing literature dealing with point distribution models, no outlier detection has been introduced. Typically, when using PDM’s, shapes that do not correspond to the allowed shape at any stage of the detection process are rejected (Fig. 1).

To treat the problem of outliers in a systematic fashion, an approach to outlier detection and position adjustment was developed. The misplaced points are identified using the information about the relative positions of the shape model vertices that are implicitly included in the shape model. Let $z = (x', y')^T$ be the model point positions after the piecewise linear transforms were applied and the resulting shape was aligned with the shape average. According to the shape model, the hypothesized shape should satisfy $\mathbf{z} = \bar{\mathbf{x}} + P\mathbf{b}$ where $\bar{\mathbf{x}}$ is the average shape, P is the matrix of the first t eigenvectors, and \mathbf{b} is a vector of

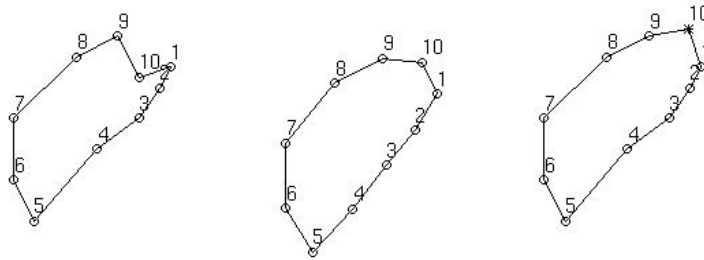


Fig. 1. Example of a shape hypothesis rejected by the Cootes' ASM procedure (left). Note the one outlier responsible for rejection (marked by 10). The same shape hypothesis after our outlier removal and adjustment steps (right, adjusted vertex marked by *). The average shape is shown in the middle.

weights. Therefore,

$$b_j = \sum_{i=1}^n P_{i,j}(z_i - \bar{x}_i) = \sum_{i=1}^n v_{i,j} \quad (1)$$

where

$$|v_{i,j}| = |P_{i,j}(z_i - \bar{x}_i)| \quad (2)$$

is the absolute variation induced by point i in parameter b_j . Let the percentage of variation induced by point i in parameter b_j be defined as

$$V_{i,j} = \frac{|v_{i,j}|}{\sum_{i=1}^n |v_{i,j}|} 100 \quad (3)$$

and let the maximum percentage of variation induced by point i in any of the parameters b_j be defined as

$$u_i = \max_{j=1..t} V_{i,j} \quad (4)$$

If all the points were to generate an equal amount of variation, then all the percentages u_i were approximately $100/n$, n being the number of object points. However, since outliers may be present, larger variation may be associated with some points – the outliers. A point is considered to be an outlier if the percentage of variance generated by its position in any of the parameters b_i of the model is more than $4 \times$ greater than the average amount of variation. If several outliers are present, the variance is distributed among them and (perhaps) the well placed points. As a result, it is difficult to identify outliers if more than a few occur simultaneously. Once such misplaced points are detected, they must be moved to a new position that can be inferred from the alignment of the rest of the shape instance with the average shape.

Final point adjustment Some of the shape model points may have been declared outliers in the previous step. Consequently, their position may have been

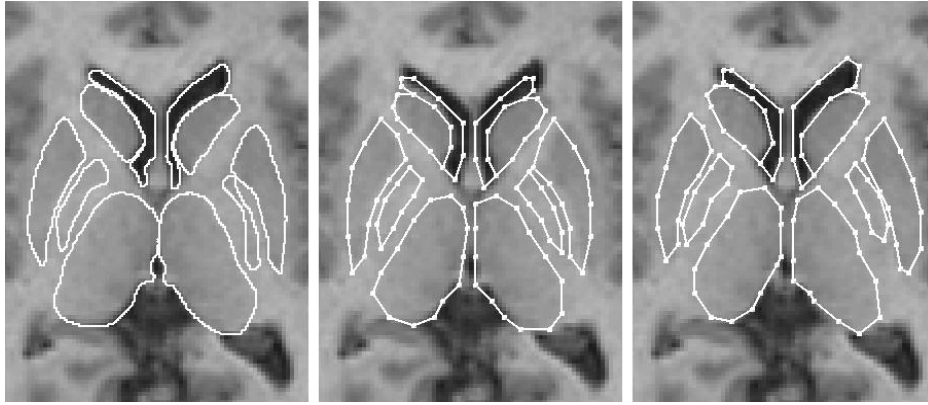


Fig. 2. Example of automated brain image segmentation and interpretation. From left to right: Manual tracings. Initial average position of the shape model. Automated segmentation.

adjusted solely considering the average shape appearance and not considering the image data. Therefore, they must be subjected to the position optimization step to better correspond with the image data.

Final outlier removal Resulting from the previous steps or newly introduced during the final point adjustment, outliers may remain present in the shape model. Following the same outlier detection procedure applied in the first outlier removal step, the outliers are identified and removed, no adjustment is attempted in this final step of model fitting.

3 Experimental Methods

The method presented above was employed to design a PDM shape model for ten neuroanatomic structures: left/right ventricles, left/right caudate nucleus, left/right putamen, left/right globus pallidus, left/right thalamus.

The knowledge-based PDM image interpretation method was tested in in vivo MR brain images. The image set consisted of individual T1-weighted contiguous MR images of the human brain, imaged in the coronal plane and acquired from a GE 1.5 Tesla Signa scanner with in-slice resolution of 256×256 pixels, slice thickness 1.5 mm, and a field of view of 26 cm. The images were acquired from 27 subjects and “normalized” using a three-dimensional proportional Talairach grid system.

Observer-defined contours identified by a neuroanatomist were available for all the images in the brain data set. However, a subset of 8 images from this set, called the training set, served for the shape model construction. The remaining 19 images formed the test set that was used for validation.

Performance of the PDM approach to image interpretation was assessed in the test set by quantitatively comparing the labels, areas, and border positions

of identified neuroanatomic structures with those determined by the observer-defined independent standard. Signed area error, labeling error and border positioning error were used as measures for comparing the observer-defined and computer-determined contours of neuroanatomic structures. The calculated indices were identical to those previously employed in [3].

4 Results

The PDM approach to brain image segmentation and interpretation correctly interpreted the brain neuroanatomic structures in all images from the test set. Fig. 2 shows the observer-traced and computer-detected contours. In the test set, the neuroanatomic structures were identified with the signed percent area error of $12 \pm 5\%$ and labeling error of $7 \pm 3\%$. Border positioning errors were quite small, with the average border positioning error of 0.8 ± 0.1 pixels, and maximum border positioning error of 4.3 ± 1.2 pixels. The detection time was about 3 minutes using a combination of C and MATLAB running on an HP 750 workstation.

5 Conclusion

A new fully automated segmentation and interpretation method has been presented in which a novel outlier-detection approach was successfully utilized. Compared to our previously-reported brain image segmentation and interpretation approach [3], our new method described here offers comparable segmentation and interpretation performance while the speed of the interpretation process has increased thirty times.

Acknowledgments

The authors wish to express their thanks to Nancy Andreasen, M.D., Ph.D., Michael Flaum, M.D., Rajprabhakar Rajarethinam, M.D.; and Ted Cizadlo, M.S. for providing both original and manually-traced MR brain data utilized in the presented study. Computer facility support of Prof. George Stockman after N. Duta moved to the Michigan State University is also gratefully acknowledged. This work was supported in part by the NSF grant IRI 96-16747.

References

1. T F Cootes, A Hill, C J Taylor, and J Haslam. Use of active shape models for locating structures in medical images. *Image & Vision Computing*, 12(6):355–366, 1994.
2. T F Cootes, C J Taylor, D H Cooper, and J Graham. Active shape models – their training and application. *Computer Vision and Image Understanding*, 61:38–59, 1995.
3. M Sonka, S K Tadikonda, and S M Collins. Knowledge-based interpretation of MR brain images. *IEEE Trans. Med. Imaging*, 15:443–452, 1996.